MANCHESTER 1824
The University of Manchester

The University of Manchester Research

Interactions of hydrogen atoms with boron and gallium in silicon crystals co-doped with phosphorus and acceptors

DOI:
10.1016/j.solmat.2023.112447

Document Version
Accepted author manuscript

Link to publication record in Manchester Research Explorer

Citation for published version (APA):
Fattah, T. O. A., Markevich, V. P., Gomes, D., Coutinho, J., Abrosimov, N. V., Hawkins, I. D., Halsall, M. P., & Peaker, A. R. (2023). Interactions of hydrogen atoms with boron and gallium in silicon crystals co-doped with phosphorus and acceptors. *Solar Energy Materials and Solar Cells*, *259*, Article 112447. https://doi.org/10.1016/j.solmat.2023.112447

Published in:
Solar Energy Materials and Solar Cells

Citing this paper
Please note that where the full-text provided on Manchester Research Explorer is the Author Accepted Manuscript or Proof version this may differ from the final Published version. If citing, it is advised that you check and use the publisher's definitive version.

General rights
Copyright and moral rights for the publications made accessible in the Research Explorer are retained by the authors and/or other copyright owners and it is a condition of accessing publications that users recognise and abide by the legal requirements associated with these rights.

Takedown policy
If you believe that this document breaches copyright please refer to the University of Manchester's Takedown Procedures [http://man.ac.uk/04Y6Bo] or contact uml.scholarlycommunications@manchester.ac.uk providing relevant details, so we can investigate your claim.

Download date:25. Mar. 2025

Interactions of Hydrogen Atoms with Boron and Gallium in Silicon Crystals co-doped with Phosphorus and Acceptors

Tarek O. Abdul Fattah,[a*] Vladimir P. Markevich,[a] Diana Gomes,[b] José Coutinho,[b] Nikolay V. Abrosimov,[c] Ian D. Hawkins,[a] Matthew P. Halsall,[a] and Anthony R. Peaker [a]

[a] *Photon Science Institute and Department of EEE, the University of Manchester, Manchester M13 9PL, United Kingdom*

[b] *Department of Physics and I3N, University of Aveiro, Campus Santiago, 3810-193 Aveiro, Portugal*

[c] *Leibniz-Institut für Kristallzüchtung (IKZ), Max-Born-Straẓe 2, 12489 Berlin, Germany*

** Corresponding author:*

Email address: tarek.abdulfattah@postgrad.manchester.ac.uk

Abstract: Reports showing that hydrogen and group-III acceptors play an important role in Light and elevated Temperature Degradation (LeTID) of Si-based solar cells highlight the need for a better understanding of interactions between these two species. In this contribution, a combination of junction spectroscopy techniques and first principles modelling has been used to study hydrogen-induced changes in electrical properties of either boron or gallium Czochralski-grown silicon co-doped with phosphorus in order to produce n-type material facilitating novel techniques to assess recombination active defects. The interactions of hydrogen with acceptor atoms have been induced via annealing of these co-doped hydrogenated samples with the application of reverse bias (RBA). These treatments have resulted in significant increase in the net shallow donor concentration in depletion regions of both materials and in the appearance of a strong electron emission signal due to a trap with an energy level at about E_c-0.18 eV in the DLTS spectra of Si:P+B material. It is argued that this trap is related to the donor level of a BH_2 complex. Calculations using density functional theory have shown that the BH_2 defect has a charge-state dependent geometry, which turns out to be crucial for the proposed non-radiative recombination mechanism. The BH_2 defect is therefore suggested to be the root cause of LeTID in boron-doped Si. In contrast, modelling results predict that GaH_2 is a defect with shallow energy levels, without the characteristic features of a recombination centre. This is corroborated by the results of electrical measurements on hydrogenated Si:P+Ga subjected to RBA. Conventional annealing treatments were subsequently used to assess the thermal stability of acceptor-H related defects. Based on the obtained results, the peculiarities of hydrogen interactions with boron and gallium acceptors are discussed.

Keywords:

LeTID, lifetime degradation, silicon solar cells, hydrogen, DLTS, acceptor-hydrogen interaction

1. Introduction:

The rapid penetration of Ga-doped Czochralski-grown Si material into the PV market has been motivated by the suppression of degradation associated with acceptor-oxygen defects using established cell manufacturing processes [1, 2]. However, instabilities of electrical performance of Ga-doped Si material related to other degradation mechanisms have not been studied extensively. A number of contradictory observations about the stability of Ga-doped Si solar cells have increased in

recent years, especially in consideration of light and elevated temperature induced degradation (LeTID). The initial thought was that Ga-doped Si material offers better stability against LeTID compared to B-doping [3], but this was then proved to be inaccurate in the light of the observations of noticeable levels of degradation of Si:Ga PERC solar cells [4, 5]. Even though Ga-doped Si wafers experience slower degradation compared to B-doped ones at the same illumination conditions [6], the formation of LeTID defect in Ga-doped Si material in densities as high as those found in B-doped Si material can be triggered by illumination with low injection levels [7]. Another recent study has shown the occurrence of light induced degradation due to acceptor-oxygen reactions (LID) in Ga-doped Si material, thus opposing the common opinion that this material is LID-resistant [8].

In consequence, the efforts invested in understanding and suppressing LeTID have been extensive because of the need for high efficiency and stable solar PV cells in the future green energy mix. The body of literature on LeTID provides many insights about the impact, key behaviour and conditions of occurrence of this mechanism in different Si materials, but as yet, there is no agreement on the root causes of LeTID and even less information is available on the composition of the defect responsible for it [9]. The involvement of hydrogen in the occurrence of LeTID has been manifested in a number of experiments which are known to affect the concentration and/or the dynamics of hydrogen in the silicon bulk, including contact firing profiles [10-12] , passivation layer properties [13-15], and wafer thickness [16, 17]. Another important observation to mention is the occurrence of LeTID in different kinds of Si materials, making it a universal degradation process [10, 18].

Understanding the behaviour of hydrogen in silicon is a key prerequisite to revealing the full story of LeTID. The cooling down of fired silicon solar cells to room temperature causes the transformation of hydrogen from isolated ions mostly to hydrogen dimers (H_2) at tetrahedral interstitial sites (T), which can be stabilized at room temperature at T sites close to some abundant impurities, e.g. oxygen in Czochralski-grown (Cz) Si. The H_2 interactions with other impurities such as the formation of BH pairs in B-doped silicon are induced via annealing treatments at temperatures higher than 100 ^{o}C. Several groups attempted to relate the observable changes in resistivity (due to BH pair formation/dissociation assuming the consumption of one hole by each created pair) to the changes in the LeTID defect density and kinetics [19-21]. In B-doped silicon, the material on which most of the previous studies have been conducted, the understanding of reaction dynamics and exchange between BH and H_2 in correlation to LeTID and the role of holes is further complicated by the potential existence of different types of hydrogen dimers [22, 23], and by the confusion with BO-LID regeneration which has been also correlated to the dissociation of BH pairs [24].

More importantly in the current context, LeTID is influenced by the nature of dopant species, which seem to play an important role in the formation/dissociation of the recombination active defects [7, 25]. The reactions governing LeTID are affected by the properties of the dopant atoms, which possibly induce changes into the hydrogen-acceptor interactions in the material. The transition to Ga-doped silicon as a PV material of choice, also raises the question of how atomic and dimeric hydrogen behaves in this material. Several questions can be raised at this point: what is the difference in the interaction of hydrogen with Ga compared to that with B? Can the peculiarities of LeTID in B- and Ga-doped silicon be explained if details of the H-acceptor interactions are known? Generally speaking, results of the assessment of the stability of Ga-doped silicon are not understood. It has been reported that wafers from different ingots with similar specifications behave quite differently and even wafers from the same ingot can respond differently to LeTID treatments [1].

It has been recently proposed that the occurrence of LeTID in boron-doped Si is related to the formation of boron-dihydrogen complex (BH_2), which forms upon hydrogen introduction and interaction with boron atoms [26]. The complex has a donor level at about 0.175 eV below the

conduction band and has a large capture cross section for minority carriers in p-type Si. This assignment makes it interesting to compare the interactions of hydrogen atoms with Ga and with B acceptor atoms which are the two dominant p-type dopants.

2. Experimental and Modelling details:

The wafers used in this study were cut from n-type ingots co-doped with phosphorus and either boron or gallium, which were grown at the Leibniz-Institut für Kristallzüchtung (IKZ) in Berlin by the Czocharlski technique. The two grown ingots were intended to achieve a similar concentration of phosphorus of ~ 3×10^{16} cm^{-3} and concentrations of ~2×10^{16} cm^{-3} and ~1×10^{16} cm^{-3} of boron and gallium, respectively, in the Si:P+B and Si:P+Ga cases. Test growth has been performed first on single-doped ingots to optimize the growth conditions to achieve the intended concentration profiles, after which growth of the co-doped ingots was carried out. The difference in the segregation coefficients between the two involved species in each ingot leads to some variations in the concentration profiles along the length of the ingot. Both ingots have been grown in the same crucible and thus possess similar oxygen and carbon content of about 6.5×10^{17} cm^{-3} and 5×10^{16} cm^{-3}, respectively, as determined via infrared absorption measurements.

Some of the wafers were lapped to remove the surface cutting damage. The wafers were then cleaned prior to etching in a solution of potassium hydroxide (KOH) at 70°C for 10 minutes followed by a gentle second etching treatment in a mixture of hydrofluoric acid and nitric acid (HF:7HNO_3) for a few tens of seconds. Samples were then dipped in dilute (10%) HF before hydrogenation.

Hydrogenation of all samples has been achieved by diffusion of hydrogen into the samples via treatments in remote hydrogen plasma at room temperature for 30 minutes where the RF power, the chamber pressure and hydrogen gas flow rate used were 50 W, 1-2 mBar and 200-250 cc/min, respectively.

Hydrogenated samples were then processed in a thermal evaporator using gold and aluminium on the hydrogenated and back surfaces to create the Schottky and Ohmic contacts, respectively. The circular gold Schottky diodes were 1 mm in diameter. The quality of the created diodes was evaluated via conventional current-voltage (IV) measurements where the best diodes with leakage current less than 1 µA at -10 V were selected for further measurements. The capacitance-voltage (CV) technique was used to determine the concentration of uncompensated active donor atoms $N_{D\ \mathrm{active}}^{+}(W)$ in the probed region, which corresponds to the difference in concentrations of the total electrically active P atoms and the total compensating acceptor atoms (B or Ga) as a function of the depth within the probed depletion region. Deep level transient spectroscopy (DLTS) and Laplace DLTS (LDLTS) have been conducted to monitor and characterize deep level defects in the diodes [27]. CV and DLTS measurements were carried out on Schottky diodes fabricated on the hydrogenated samples and repeated after subjecting them to annealing at 100 °C for 20 minutes with an applied reverse bias of U_b=-9 V, a treatment referred to as reverse bias annealing (RBA). Subsequent measurements were also carried out after subjecting diodes to conventional annealing at temperatures in the range of 270-340 K.

Modeling of BH_n and GaH_n complexes in Si ($n = 1$, 2) was carried out within density functional theory (DFT) as implemented in the VASP package [28, 29]. The method employs the standard computational machinery of a planewave DFT code, including projector-augmented wave pseudopotentials [30] to account for core states, and planewaves (with kinetic energy of up to $E_{\mathrm{cut}} = 400$ eV) to describe the valence states. Electronic interactions were treated using the hybrid functional of Heyd, Scuseria and Ernzerhof (HSE06) [31]. This mixes a short-range exact exchange

formulation with a semi-local exchange-correlation potential [32]. The numerical accuracy attained for the total electronic energy was 10^{-6} eV.

Defects were inserted in cubic supercells made of 512 Si atoms with theoretical lattice parameter $a = 5.4318$ Å. Forces and defect geometries were found within the generalized gradient approximation [32]. After that, a final self-consistent energy calculation was carried out within hybrid DFT. The large 512 atom cells allowed us to sample the Brillouin zone at the Γ-point. A few tests were conducted using $2 \times 2 \times 2$ grids of $\mathbf{k}$-points to validate the geometries. Energies of non-zero charge states include a periodic charge correction [33].

We also investigated reaction energies and their energy barriers. For a specific reaction $X \rightarrow Y$, the binding energy is the opposite of the reaction energy, $E_{\mathrm{b}} = -\Delta E_{\mathrm{R}} = E_X - E_Y$, and the activation energy is $E_{\mathrm{a}} = E^{\ddagger} - E_X$. Here, E_X and E_Y are energies of reactants and products (with identical stoichiometry), while $E^{\ddagger}$ is the energy of the transition state. The latter was found using the nudged elastic band method with 64-atom supercells, and a sequence of 11 geometries along the mechanism.

For reactions involving the capture or emission of free carriers, we must also account for the energy of the carriers when they occupy conduction band bottom states (electrons) or valence band top states (holes). For instance, for $X^0 \rightarrow X^- + \mathrm{h}^+$ the energy of the products is obtained as $\tilde{E}(X^-) + E_{\mathrm{corr}}(X^-) - \varepsilon_{\mathrm{v}}$. The first two terms represent respectively the energy of the ionized defect as computed from the periodic supercell and respective charge correction. The subtraction of an electron from the valence band top (free hole) is accounted for by the third term, which is the energy of the highest occupied Kohn-Sham state of a bulk calculation. Conversely, the energy of a free electron is that of the lowest unoccupied Kohn-Sham state in bulk Si. Further details of the method are available in Ref. [34].

3. Results and Discussion

3.1 Modelling of hydrogen interactions with boron and gallium

The reaction $A^- + \mathrm{H}^+ \rightarrow A\mathrm{H}$, where reactants comprise a bond centred proton infinitely separated from a substitutional ionized acceptor, is highly favourable due to combined long range Coulomb attraction and fast diffusivity of hydrogen. The resulting acceptor-hydrogen pair ($A\mathrm{H}$) is depicted in Fig. 1 for the case of BH and GaH. A Si-H bond is drawn (and there is no A-H bond), emphasizing that a covalent bond is established between Si and H, while the acceptor is three-fold coordinated [35]. The energy of the reactants was found from two independent supercell calculations.

According to recent results, the potential energy barrier for migration of H^+ amounts to 0.42 eV [34]. This is represented in Fig. 1 as a black line on the right-hand side of the reaction coordinate diagram. The figure also depicts the reaction energies of first, second, and third neighbouring $A\mathrm{H}$ pairs (negative values next to the minima), as well as barriers that connect them (positive values next to the arrow heads).

The first dissociating jump of hydrogen away from B has a calculated activation energy of 0.98 eV. Considering the relative energies of first and second neighbouring B-H pairs, we find that the largest barrier that H^+ must surmount before BH formation, occurs in the last jump before paring, and is about 0.7 eV. The reason for such a pronounced barrier stems from a relative difficulty in breaking the rather short Si-B bond. Such a *capture* barrier was not found for the $\mathrm{Ga}^- + \mathrm{H}^+ \rightarrow \mathrm{GaH}$ reaction. In this case, strain around the acceptor is much weaker, and the barriers for the last two jumps of H^+ towards Ga atom are $\lesssim 0.4$ eV. The magnitude of the above barriers suggests that the presence

of free H^+ in B-doped Si, leads to formation of BH pairs around room temperature and above, whereas in Ga-doped Si the GaH pairs can be formed well below room temperature.

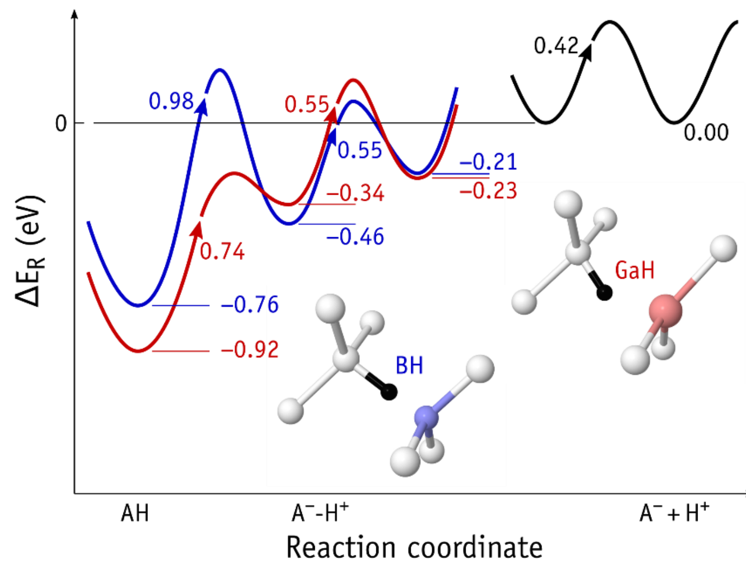

Fig. 1. Calculated reaction coordinate diagram of for $A^- + H^+ \rightarrow AH$ reaction with A standing for substitutional boron (blue) or gallium (red). The black curve represents the migration of H^+ away from the acceptor. Energies of energy minima are indicated with respect to the state of infinitely separated reactants (zero energy). Activation energies for H jumps to second and third neighbouring bonds to the acceptor, are shown next to the arrows. In the atomistic models, B, Ga, H and Si are shown in blue, red, black, and white, respectively.

The calculated binding energy of BH (0.76 eV) is lower than that of GaH (0.92 eV). This points to a higher stability of the latter pair. In Ref. [35], we argue that the reason behind the higher binding energy of GaH is not related to the specifics of the chemistry between H and the acceptors. Instead, H establishes a covalent bond to Si, the A-H interaction being mostly steric. The lower E_b for BH is due to the relatively stronger and shorter B-Si bonds, one of each must be broken in the reactants side of $A^- + \mathrm{H}^+ \rightarrow A\mathrm{H}$.

In p-type Si, acceptor-dihydrogen complexes ($A\mathrm{H}_2$) were found stabilized in the positive charge state. The ball-stick diagrams of the minimum-energy configurations of the $A\mathrm{H}_2^+$ complexes are shown in Fig. 2. Their formation is likely to proceed according to two different routes: (a) in the presence of mobile protons, which can be captured by existing $A\mathrm{H}$ pairs, $\mathrm{H}^+ + A\mathrm{H} \rightarrow A\mathrm{H}_2^+$ [26], and (b) when hydrogen molecules are available to interact directly with the acceptors, $\mathrm{H}_2 + A^- + 2\mathrm{h}^+ \rightarrow A\mathrm{H}_2^+$. The latter reaction involves the subtraction of two free holes per $A\mathrm{H}_2^+$ complex. The binding energy of H^+ to $A\mathrm{H}$ [type (a) reaction] was found as 0.40 eV and 0.48 eV for $A = \mathrm{B}$ and Ga, respectively, while $E_\mathrm{b} = 0.83$ eV and 1.07 eV for direct capture of H_2 by B^- and Ga^- [type (b) reaction]. The latter figures reflect a strong driving force for H_2 dissociation next to the acceptors, and like the acceptor-hydrogen pairs, GaH_2^+ complexes are more stable than BH_2^+. The activation barrier for dissociation of H_2 upon reaction with B^- was calculated as $E_\mathrm{a} = 1.1$ eV. The mechanism involves the collision of the molecule with a B-Si bond. Comparing this figure with the 1.62 eV barrier for H_2 dissociation in defect-free bulk Si [34], and considering the above binding energies, we conclude that B is a catalyst for H_2 dissociation, and that BH_2 is a by-product along $\mathrm{H}_2 + 2\mathrm{B}^- + 2\mathrm{h}^+ \rightarrow 2\mathrm{BH}$. Analogous behaviour is expected for Ga-doped Si, although we did not calculate the dissociation barrier of the molecule next to Ga.

Figs.Fig. 2(a) andFig. 2(b) depict the calculated configuration coordinate diagrams for BH_2 and GaH_2 complexes in Si. The origin of the energy scale represents the $A^{-}+\mathrm{H}_2+2\mathrm{h}^{+}$ state. Only the energy minima were calculated. Transformation and capture barriers in the diagrams are only schematic. Several features are evident from the figure. (1) $A\mathrm{H}_2$ complexes are bistable, being donors when the A species is undercoordinated (referred to as "D" structure), and they are acceptors when A is over coordinated (referred to as "A" structure). (2) The neutral D state (D^0) of BH_2 is metastable, while this is the most stable configuration for GaH_2^0. (3) As referred above, the binding energies suggest that GaH_2^+ is more stable than BH_2^+. (4) BH_2^+ is a deep donor (with a calculated donor transition at $E_\mathrm{c}-0.19$ eV) and BH_2^- is a shallow acceptor comparable to substitutional boron. On the contrary, GaH_2^+ shows both shallow donor and shallow acceptor transitions. (5) Both $A\mathrm{H}_2$ complexes show a negative-U ordering of donor and acceptor levels. However, while BH_2 has a $(-/+)$ transition in the lower half of the gap (estimated at $E_\mathrm{v}+0.26$ eV), the analogous transition for GaH_2 is estimated close to mid-gap ($E_\mathrm{v}+0.61$ eV).

In Ref. [26], a sequence of reactions pertaining to the LeTID process in B-doped solar cells were proposed, where BH_2 was presented as the root cause of the life-time degradation. The calculated donor transitions suggest that BH_2^+ can be an efficient electron trap in p-type Si. However, GaH_2^+ is too shallow and cannot explain the apparent observation of LeTID in Ga-doped Si cells [4, 6, 7]. Improvements to the model, or alternative explanations have to be evoked. Possibilities include boron contamination in Ga-based cells, formation of multiple LeTID defects (possibly having H as a common constituent) under specific conditions, or formation of a lifetime limiting centre without the participation of group-III species (possibly involving the following elements: hydrogen, carbon and oxygen).

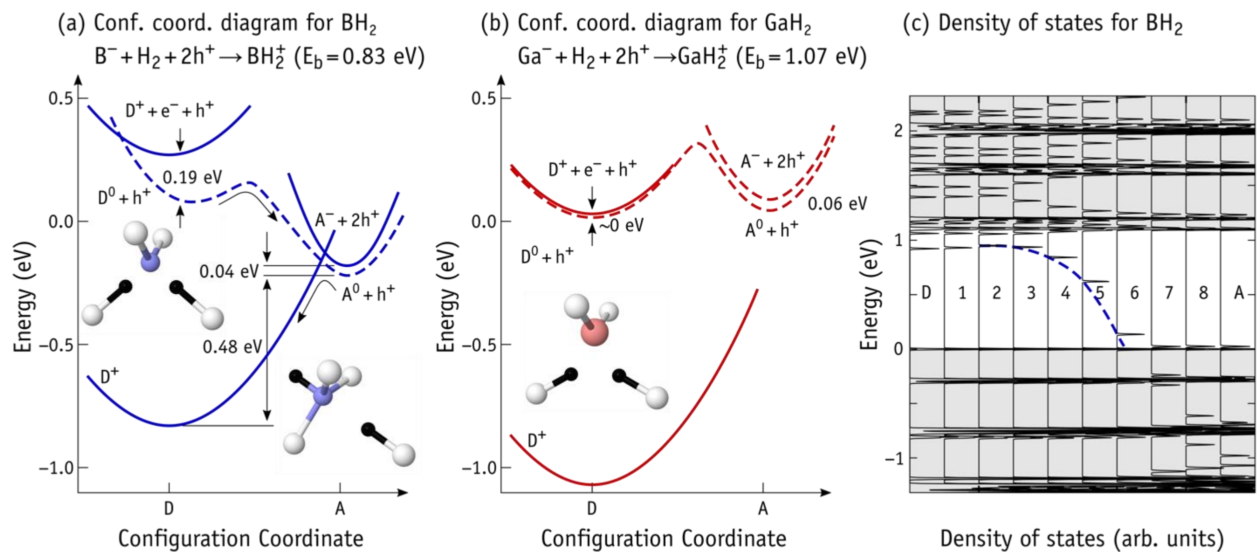

Fig. 2. Configuration coordinate diagrams for (a) BH_2 and (b) GaH_2 complexes in Si. In both diagrams the origin of the energy scale corresponds to the $A^{-}+H_2+2h^{+}$ state. (c) Shows the evolution of the electronic structure of BH_2 along the transformation $BH_2^0(D)\rightarrow BH_2^0(A)$, highlighting the position of a semi-occupied gap state responsible for electron and hole capture.

Despite the above, to succeed as a credited model, the BH_2 complex must be an efficient non-radiative recombination centre, *i.e.*, efficient at trapping both electrons and holes. The donor state of the D-form of BH_2 is far from the valence band top, and therefore unlikely to lead to efficient hole capture. We found however a possible route for sequential electron-hole capture, which proceeds in

three steps. Step 1 – capture of a photo-generated electron by D^{+}state, step 2 – structural reconfiguration $\mathrm{D}^{0} \rightarrow \mathrm{A}^{0}$, and step 3 – capture of a hole by A^{0} state. Notably, BH_{2} is not a typical Shockley–Read–Hall recombination centre with a static level near mid-gap. Instead, the high recombination efficiency is expected from its dynamic electronic structure along the three steps. Initially, the D^{+} state introduces an electron trap close to the conduction band bottom, and a large electron capture cross-section for electrons is expected. However, upon the capture of an electron, D^{0} is metastable and relaxes into state A^{0} in step 2. The defect is now a hole trap edging the valence band top, hinting for a large capture cross section for holes. After hole capture in step 3, the defect returns to the D^{+} ground state, becoming ready for another recombination cycle.

The above is better understood with the help of Fig. 2(c). In there, we depict the evolution of the electronic density of states (DOS) of a defective supercell containing a BH_2 complex in the $q = 0$ charge state. States D^{0} and A^{0} are shown on the left and right ends of the diagram. For the sake of clarity, the calculated DOS ignores spin polarization, so that the peak within the band gap (highlighted by the blue dashed line) is semi-occupied. The diagram shows that the defect state spans the whole band gap, edging the conduction band bottom in the D-form, and *plunging* into the valence band in the A-form. This feature anticipates a strong coupling of the defect state to both bands, and provided that no large capture barriers exist along (1) $\mathrm{D}^{+} + \mathrm{e}^{-} \rightarrow \mathrm{D}^{0}$, (2) $\mathrm{D}^{0} \rightarrow \mathrm{A}^{0}$ and (3) $\mathrm{A}^{0} + \mathrm{h}^{+} \rightarrow \mathrm{D}^{+}$, carrier recombination could be fast, simply involving jumps of H around boron. Preliminary calculations indicate that the barriers are as low as $\sim$0.1-0.2 eV. However, we leave further considerations for a future publication.

3.2 Effect of RBA treatment on $N_D^+(W)$ dependencies in hydrogenated diodes:

Hydrogen-related defects with deep energy levels in the gap are not necessarily formed immediately upon the introduction of hydrogen into Si, but often hydrogen interactions with several species in Si are triggered by annealing and/or injection of majority or minority carriers. In this work, the manipulation of hydrogen distribution, nature and/or interaction with other impurities have been achieved mainly via reverse bias annealing (henceforth "RBA") and conventional annealing treatments (unbiased annealing). The spatial concentration profiles of uncompensated ionized P atoms $N_D^+(W)$ in diodes made on Si:P+B and Si:P+Ga co-doped Si samples upon hydrogenation via remote H plasma are shown in Fig. *3*. The bulk uncompensated donor concentration values in both materials, as determined from CV measurements, are in agreement with the growth specifications. Close to the surface, the passivation of the electrical activity of donor atoms can be explained by the interaction of H^- atoms introduced via H plasma treatment with P^+ atoms thus forming electrically inactive PH pairs, which do not appear to introduce any energy levels in the bandgap of Si. Although the formation of PH_2 may be energetically possible, we are not aware of any experimental observation of such phosphorus related defects [36, 37].

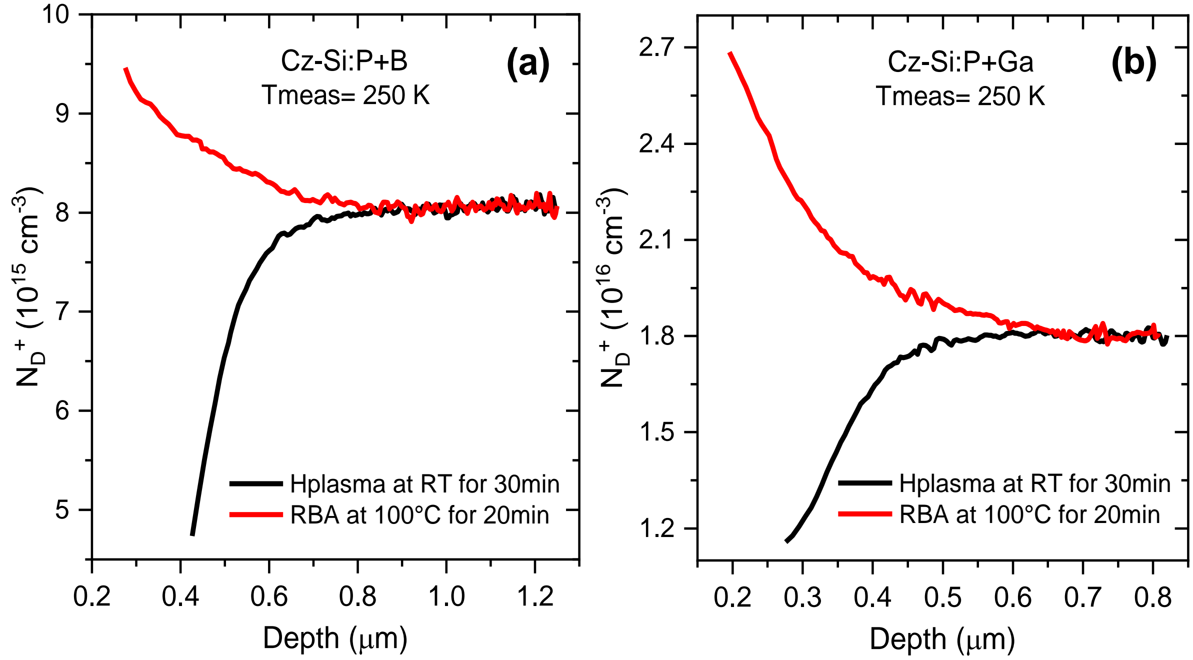

Fig. 3. Depth profiles of uncompensated shallow donor concentration, $N_D^+(W)$, in diodes fabricated on (a) Si:P+B, and (b) Si:P+Ga materials measured at 250 K after treatments in remote H plasma at room temperature and application of RBA at 100°C subsequently.

Diodes were then subjected to RBA treatments by which they are kept at 100 °C for 20 min under a reverse bias of $U_b = -9\ V$. The purpose of this treatment was to i) release the trapped hydrogen atoms from the donor atoms and ii) transform the released hydrogen to the positively charged state H^+ and allow it to drift under the bias field. Fig. 3 shows significant changes in the $N_D^+(W)$ dependencies in both materials after the RBA treatments. In the region close to the surface, a strong increase in $N_D^+(W)$ values has been observed. The values of N_D^+ close to the surface are higher than those in the deeper bulk in both materials. This can be explained by the RBA-induced interaction of hydrogen atoms with acceptor dopant atoms B and Ga in the depletion regions of Si:P+B and Si:P+Ga, respectively. Besides the increase in concentration of electrically active P^+ atoms, which have appeared after the dissociation of PH pairs, some acceptor atoms become passivated. Hence, a corresponding number of ionized B and Ga atoms which initially (after hydrogenation via H plasma) compensated the ionized P atoms, such that $N_{D\,active}^+(W) = N_{D\,total}^+(W) - N_A^-(W)$, are deactivated by hydrogen after RBA. This interaction of B and Ga with hydrogen upon RBA means that fewer impurities are available to compensate the P atoms thus increasing $N_{D\,active}^+(W)$ values close to the surface.

3.3 Effect of RBA treatment on DLTS spectra recorded on hydrogenated diodes:

The substantial effect of RBA treatments on the $N_D^+(W)$ profiles makes it important to investigate whether such treatments also introduce hydrogen-related defects signatures in the materials. For this purpose, conventional DLTS measurements were carried out on the same diodes on which the $N_D^+(W)$ dependencies shown in Fig. 3 were measured, the results of which are shown in Fig. 4.

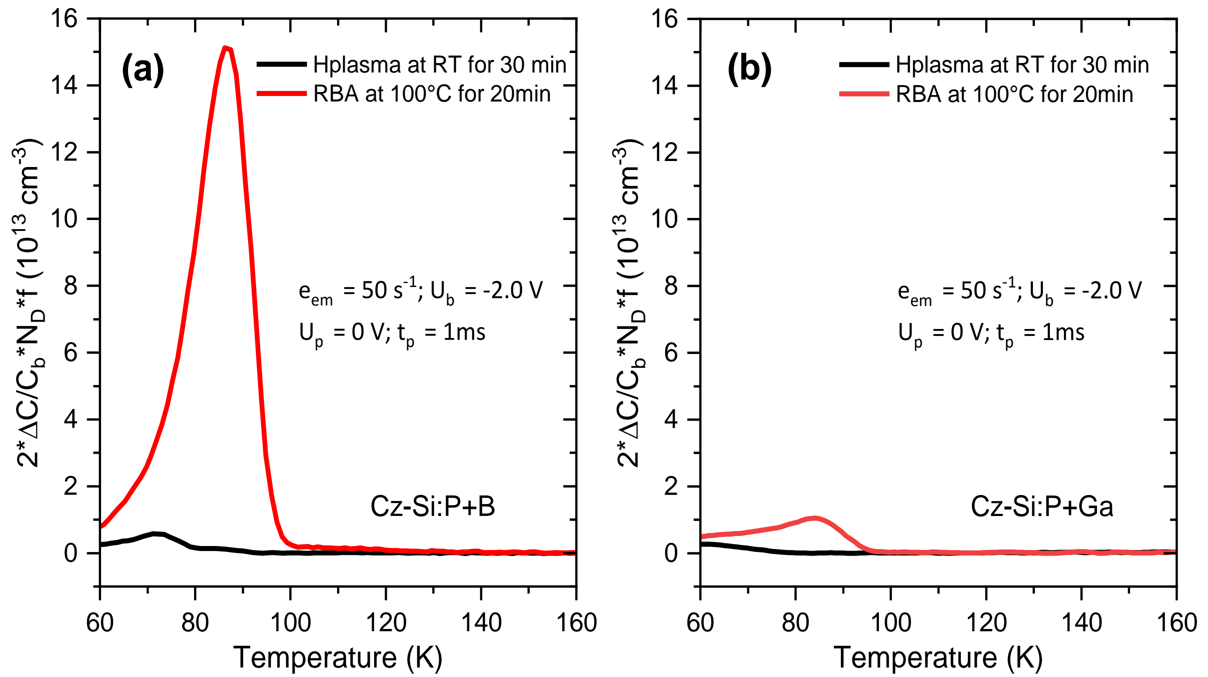

Fig. 4. Conventional DLTS spectra recorded in the temperature range 60-180 K on diodes fabricated on (a) Si:P+B, and (b) Si:P+Ga materials subjected to hydrogenation via remote H plasma at room temperature and RBA treatment at 100°C subsequently. Measurement conditions are shown in the graph.

Values on the vertical axis in Fig. *4* are $2(\Delta C/C_{\mathrm{b}})N_{\mathrm{D}}f$, where ΔC is the magnitude of a capacitance transient, C_b is the bias capacitance, and f is the correction function, which takes into account depletion widths at the bias and pulse voltages [27] . The values at the peak maxima are close to the average trap concentrations in the probed region. The spectra shown in Fig. *4* are representative of the regions from about 0.24 to 0.59 µm for Si:P+B and from about 0.18 to 0.38 µm for Si:P+Ga. The DLTS spectra recorded after hydrogenation on the same diodes on both materials in the temperature range 60-160 K show only weak electron emission signals in the temperature range 60-80 K, which have been assigned previously to carbon-hydrogen-oxygen related complexes [38-41]. Upon the application of the RBA treatment, however, a strong electron emission signal with its maximum at about 87 K and mean concentration higher than 10^{14} cm^{-3} has been detected in the diode fabricated on Si:P+B material. In the case of Si:P+Ga material, a much weaker DLTS signal has been detected approximately at the same position as that detected in the Si:P+B material spectrum.

Given that the two materials have been hydrogenated in remote H plasma under the same treatment conditions, the significant difference in the RBA-induced DLTS signals between Si:P+B and Si:P+Ga materials cannot be assigned to the difference in the hydrogen concentrations in the two materials. This is also supported by the very similar changes in $N_D^+(W)$ initially (after hydrogenation) and upon RBA. The combination of DLTS and CV results indicates that i) hydrogen interacts effectively with both B and Ga atoms upon the RBA treatment of hydrogenated samples and ii) the electronic properties of the RBA-induced H-acceptor complexes are different.

The electronic properties of the complex responsible for the strong DLTS signal with its maximum at 87 K (E_{87K} trap) has been recently studied [26]. It has been argued that a complex consisting of a boron atom and two hydrogen atoms, BH_2, is responsible for the observed DLTS peak with a donor level at ~0.18 eV below the conduction band edge. The modelling results reported above support

those findings. Such a complex has a large capture cross section for electrons and can act as an effective recombination centre for minority carriers in p-type silicon.

It has been also reported previously that RBA treatments initiates the interaction of hydrogen atoms with substitutional carbon atoms [40, 42, 43]. Thus, the possibility of assigning observed changes in the DLTS spectra to carbon-hydrogen complexes instead of acceptor hydrogen complexes has been also probed by carrying a similar study on a carbon-rich hydrogenated P-doped Si material [26]. Several observations reported by De Guzman et al. [26] and in this work support the elimination of the assignment of E_{87K} trap to the formation of C_S-H_x complexes: 1) the formation of carbon-hydrogen pairs cannot explain the increase in the uncompensated donor concentrations to values higher than the bulk value, 2) the RBA-induced increase in the DLTS peak in the temperature range 80-90 K related to carbon-hydrogen complexes in the H plasma treated C-rich P-doped Si material is not very significant and cannot account for the very high concentration of the E_{87K} trap in the Si:P+B material, 3) the presence of the boron atoms is necessary to observe the appearance of the very strong signal in DLTS, and 4) the ingots, from which both Si:P+B and Si:P+Ga wafers were cut, were grown in the same crucible and under the same growth conditions and thus the carbon concentration in both materials is very similar ($[C_S]$~$5*10^{16}$ cm^{-3}). If C_S-H_x complexes were responsible for the observed E_{87K} trap in DLTS, the same peak would have been observed in the case of the Si:P+Ga material, if not to say even stronger in the C-rich P-doped Si material containing $[C_S]>10^{17}$ cm^{-3}. Furthermore, the CH_B defect concentration profile reported in Ref. [40] shows an increase in the defect concentration followed by a decrease deeper in the bulk. This is not the case for the BH_2 defect distribution which attains maximum concentration close to the surface and constantly decreases with depth (see figure 6 in Ref. [26]). Based on these statements, the assignment of the observed DLTS signal in Si:P+B material to carbon-hydrogen complexes is ruled out.

The above discussion does not exclude the formation of carbon-hydrogen complexes in both materials. Instead, it means that their existence cannot account for the observed changes in CV/DLTS results in the Si:P+B material. In fact, the observed changes in DLTS for diodes made on Si:P+Ga material after RBA can be explained by the reported RBA-induced formation of C_S-H_x complexes in hydrogenated carbon-rich n-type Si, given that the peak amplitude is much smaller than in the case of Si:P+B. These complexes give rise to a DLTS signal with its maximum at 85-90 K and are likely to incorporate carbon and hydrogen [40]. Another potential reason for the observed signal in DLTS in the case of Si:P+Ga is the contamination with boron. If during the growth some boron content has been incorporated, it might be possible that some BH_2 complexes form in this material as well. Further investigations are needed to sustain this possibility.

The literature results and the results of our calculations show that BH and GaH complexes are electrically inactive [37, 44-47]. Therefore, the combined analysis of RBA-induced changes of $N_D^+(W)$ and DLTS spectra in both materials, leads us to propose the formation $A\mathrm{H}_2$ complexes in the depletion regions of diodes made on Si:P+B and Si:P+Ga materials, by the interaction of hydrogen atoms released from PH pairs upon RBA treatments. BH_2 is a complex possessing a donor level at ~0.18 eV below the conduction band and is responsible for a DLTS signal with its maximum at 87 K in the RBA-treated Si:P+B material. The BH_2 complex is an attractive centre for electrons and is likely to be an effective recombination centre being involved in LeTID in p-type Si. The similar changes in the $N_d^+(W)$ dependencies in hydrogenated Si:P+Ga upon RBA (Fig. 3) suggests that the Ga-H interactions are similar to B-H interactions and, thus, the formation of the GaH_2 defects in Si:P+Ga is expected. According to the calculations, GaH_2 complexes, like BH_2, are expected to form upon RBA. However, unlike BH_2, GaH_2 is a shallow donor with a level edging the conduction band bottom. This result is

consistent with the absence of a DLTS signature for GaH_2 in the P+Ga samples. The difference in the electronic properties of the two acceptor-dihydrogen complexes suggests that only BH_2 is an effective recombination centre for minority carriers (electrons) which can be formed under LeTID treatments in hydrogenated B-doped Si.

3.4 Annealing behaviour of BH_2 vs GaH_2 complexes:

3.4.1 Isothermal annealing at 290 K:

To learn more about the difference in the electronic properties of BH_2 and GaH_2 complexes, the annihilation kinetics of these complexes are studied via the application of biased and conventional (open circuit) annealing treatments, i.e. diodes heated with bias ($U_b = -9\ V$) and without bias ($U_b = 0\ V$).

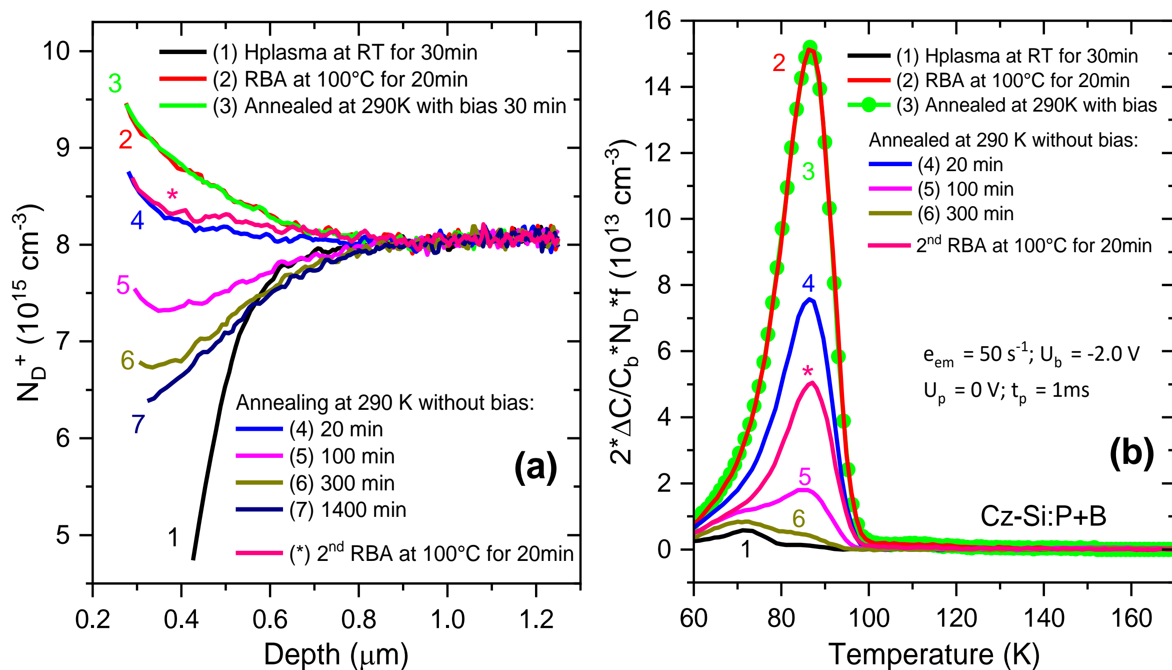

Fig. 5. (a) Spatial profiles of uncompensated donor concentration in a diode on Si:P+B sample subjected to following annealing treatments at 290 K after 1) hydrogenation via H plasma and 2) RBA at 100°C: 3) with U_b= -9 V for 30 min and without bias for a cumulative duration of 4) 20 min, 5) 100 min, 6) 300 min and 7) 1400 min. The spatial profile of $N_D^+(W)$ recorded on the same diode after a 2nd RBA treatment applied subsequently after annealing treatments is also shown by the asterisk. (b) DLTS spectra recorded on the same diode after each of the aforementioned treatment excluding the 1400 min annealing one.

The diode on the Si:P+B material was subjected to biased and unbiased annealing treatment at 290 K for 30 and 20 minutes respectively, subsequently after the RBA treatment. The changes in the $N_D^+(W)$ dependencies upon these treatments are shown in Fig. 5(a), where the results presented in Fig. 3(a) are replotted as well for the sake of comparison (lines no. 1 and 2). Annealing the diode with bias at 290 K (line no. 3) induces no changes to the $N_D^+(W)$ profile. However, a reduction in the active donor concentration close to the surface (W<0.7 μm) is observed when the bias is removed (line no. 4). The DLTS spectra recorded after each of these subsequent treatments, shown in Fig. 5(b), also reveal that the E_{87K} trap magnitude is unchanged when the annealing is done with bias but is significantly reduced when the bias is removed compared to the data recorded immediately after

RBA. These observations indicate that the donor state of the BH_2 complex disappears at 290 K only when electrons are available.

Subsequently, unbiased annealing treatments at 290 K are applied in steps, each time recording CV and DLTS after the treatment. Fig. 5(a) shows the continuous reduction in the concentration of active donor atoms upon keeping the diode for a longer time at 290 K (lines no. 5-7). The reduction in $\mathrm{N_D^+}$ values is also projected in DLTS by the continuous reduction of E_{87K} trap magnitude, which nearly disappears after keeping the diode at 290 K for longer than 300 minutes. The important message from the comparison of CV and DLTS results upon annealing the diode on Si:P+B is that changes in the DLTS signal magnitude of the E87K trap are only observed when the annealing treatment induces changes in the $N_D^+(W)$ profiles in the probed region. This further confirms that the defect responsible for DLTS signal is related to the interaction of hydrogen with B atoms monitored via the analysis of $N_D^+(W)$ plots. Analysis of the annealing-induced changes in the $N_D^+(W)$ profiles suggests the dissociation of BH_2 defects and the appearance of mobile H^- atoms upon unbiased annealing at 290 K. The H^- atoms further interact with phosphorus atoms leading to formation of PH pairs as indicated by the bowing down of the $N_D^+(W)$ profiles in the subsurface region.

If the diode is further kept at 290 K for relatively long time, i.e. >1000 minutes, the observed reduction in the $N_D^+(W)$ profile seems to saturate and does not fully recover to the as-hydrogenated state. This interesting observation can be explained by the loss of some hydrogen atoms during the reversible relocation between BH_2 complexes and PH pairs. It looks like having no electric field to preserve hydrogen close to the surface during conventional annealing can allow some hydrogen to diffuse in all directions. This is supported by the slight decrease in the $\mathrm{N_D^+(W)}$ values in the range 0.6-0.8 μm in Fig. 5(a) after annealing for relatively long time (300 and 1400 minutes) where hydrogen released from boron can capture available electrons and interact with positively charged donor atoms. To ascertain the loss of some hydrogen, a second RBA treatment has been applied to the same diode following the 1400 minutes annealing. Fig. 5(a) and Fig. *5*(b) shows that the 2nd RBA treatment (line labelled with asterisk *) has similar effect on both the $\mathrm{N_D^+(W)}$ profiles and the DLTS spectra as the effect induced by the 1st RBA treatment. Interestingly, however, the magnitudes of the observable changes are weaker this time. This further supports the proposal that some hydrogen content has been lost during the first RBA-annealing cycle.

Similar annealing treatments with and without bias have been applied to the diode on Si:P+Ga material at 290 K. The changes in $\mathrm{N_D^+(W)}$ dependencies and DLTS spectra upon these treatments are shown in Fig. 6(a) and Fig. *6*(b), respectively.

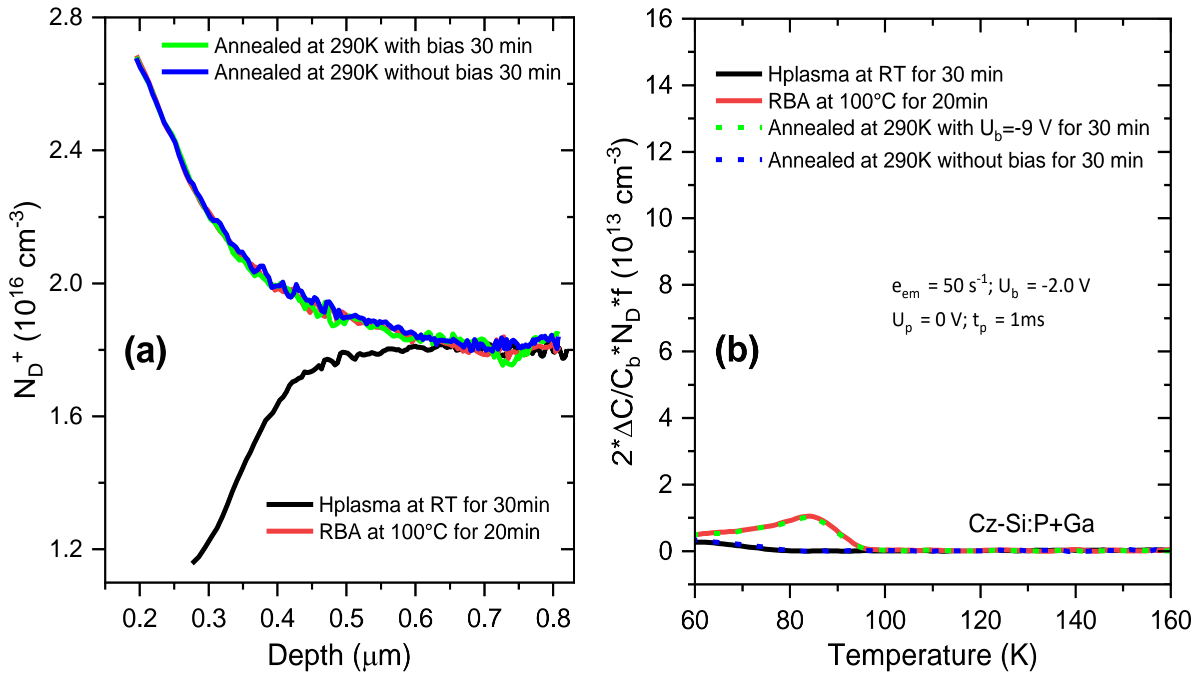

Fig. 6. (a) Spatial profiles of uncompensated donor concertation in a diode on Si:P+Ga sample subsequently subjected to 1) hydrogenation via H plasma, 2) RBA at 100°C and annealing at 290 K for 30 min 3) with bias of U_b= -9 V and 4) without bias. (b) DLTS spectra recorded on the same diode after each of the aforementioned treatment.

Similar to the BH_2 complex case, annealing the diode on Si:P+Ga material with bias induces no changes in either the $N_D^+(W)$ profile or the DLTS spectrum. In contrast to the BH_2 case, annealing the same diode without bias for the same duration causes the complete disappearance of the DLTS signal induced by RBA, but still has no effect on the $N_D^+(W)$ profile. The substantial difference between CV and DLTS results upon conventional annealing treatments importantly provides evidence that the RBA-induced changes in $N_D^+(W)$ profile are not related to the same complex as the one responsible for the weak DLTS signal. The disappearance of the weak DLTS peak after annealing at 290 K is comparable to the annealing behaviour of the carbon-hydrogen complex reported by Endrös el al. [43] and thus, supports the assignment of this peak to carbon-hydrogen related defects formed upon RBA. Several conclusions can be drawn out of these observations: 1) the presence of electrons is necessary to dissociate the BH_2 complex responsible for the E_{87K} trap at 290 K, 2) the GaH_2 complex does not introduce any DLTS signatures in the studied temperature range, 3) the GaH_2 complex is more stable than the BH_2 complex and its dissociation is extremely slow at 290 K (time scale of days-weeks).

3.4.2 Isothermal annealing of GaH_2 at 340 K:

It is only when the unbiased annealing temperature is increased to 340 K that a decrease in $N_D^+(W)$ is observed. Fig. 7(a) shows the $N_D^+(W)$ profiles on the same diode made on Si:P+Ga material after keeping it at 340 K for a cumulative duration of 20, 60, 100 and 300 minutes.

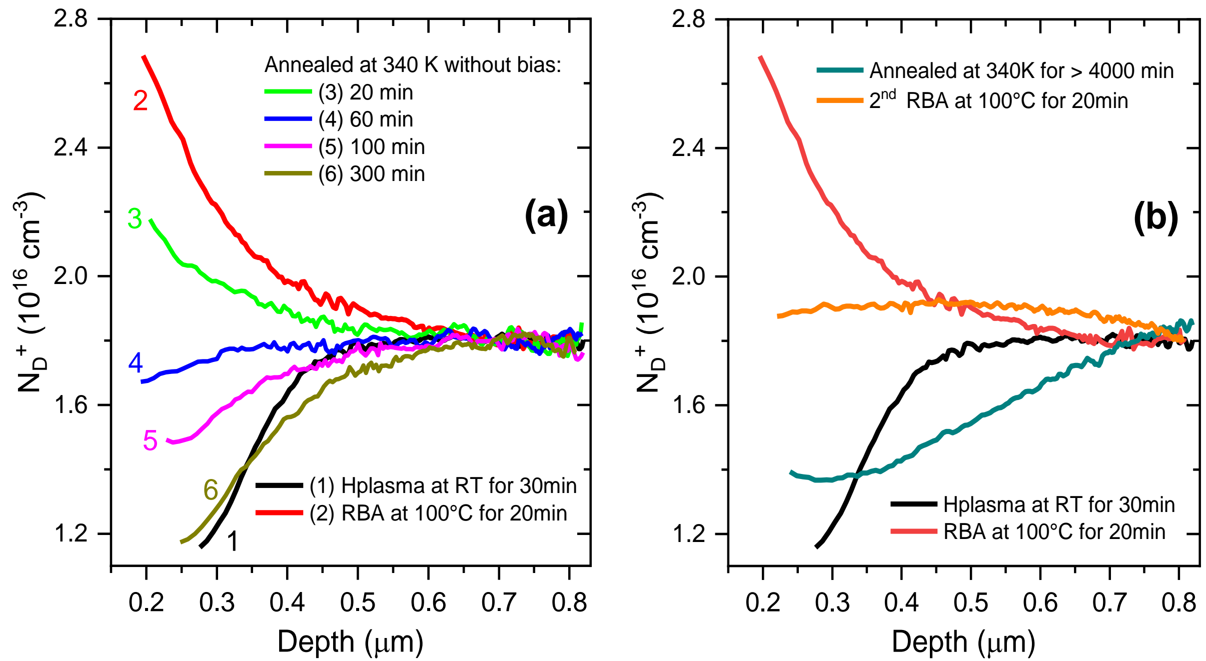

Fig. 7. (a) Spatial profiles of uncompensated donor concentration in a diode on Si:P+Ga sample subjected to conventional annealing treatments at 340 K after 1) hydrogenation via H plasma and 2) RBA at 100°C for a cumulative duration of 3) 20 min, 4) 60 min, 5) 100 min, 6) 300 min. (b) $N_D^+(W)$ profiles on the same diode shown in a) after annealing at 340 K for > 4000 min and subsequently after 2nd RBA at 100°C.

A continuous decrease in the N_D^+ values can be observed in the subsurface region for W < 0.6 µm. This can be explained by the dissociation of the GaH_2 complex when both electrons and enough thermal energy are present, similar to the effect observed for the BH_2 case at 290 K. The $N_D^+(W)$ profile after annealing the sample for 300 minutes is similar to the one recorded immediately after hydrogenation and before the application of any treatments, apart from some changes in the range 0.35 <W< 0.6 µm caused by the diffusion of released hydrogen into the bulk and interaction with P atoms. At the moment, it is not clear what caused an approximately full recovery of the as-hydrogenated profile in the case of Si:P+Ga material but not in the Si:P+B material. It looks like enough hydrogen is still present to interact with P atoms after being released from GaH_2 complexes, even if some hydrogen has been redistributed to the bulk and/or surface regions. The concentration of compensating impurities is higher in the case of Si:P+B material compared to Si:P+Ga which could mean that more trapping sites are available for hydrogen. Considering the modelling results which predict a higher stability of the A^- state of BH_2 in comparison to that of GaH_2, we may speculate that a fraction of BH_2^- complexes are still preserved after the 290K annealings in the shallow acceptor state. The full recovery effect has not been observed on another diode on a second sample of Si:P+Ga material subjected to similar treatments, but rather non-full recovery similar to observation in the case of Si:P+B material. This is currently under further investigation on more samples.

If the sample is kept for a long time at 340 K under open circuit conditions, i.e. for > 4000 minutes, the available negatively charged H^- atoms are redistributed by diffusion to the bulk region where they interact with P atoms causing the bulk donor concertation to decrease and that close to the surface to slightly recover, as shown in Fig. 7(b) which shows the long anneal with data from Fig. *7*(a) included for clarity of comparison. This effect will continue as long as the thermal energy is applied until almost uniform $N_D^+(W)$ profile is obtained.

As for the Si:P+B case, the diode on the Si:P+Ga sample was subjected to a second RBA after the prolonged annealing treatment. This time, the RBA treatment has also resulted in the recovery of the uncompensated donor concentration, but similar to the case of Si:P+B material, to a much less extent. The very long annealing time (~ 3 days) in this case prior to the 2nd RBA treatment has a negative effect on the hydrogen content close to the surface available to interact with Ga atoms upon RBA which could have penetrated very deep in the bulk beyond the probed region. The same sequence of treatments (hydrogenation-1st RBA-annealing for 300 min at 340 K- 2nd RBA) performed on another sample, without the very long annealing step, has shown very similar trend to the one observed in the case of Si:P+B material. It looks like some hydrogen has been consumed by other routes, other than the reversible formation of XH_2 (X=B or Ga) and PH complexes, upon the prolonged annealing treatments as will be discussed later.

3.4.3 Isochronal annealing of BH_2 complex:

To evaluate the temperature dependent annealing behaviour of the E_{87K} trap, Laplace DLTS measurement were carried on a diode on the Si:P+B material at 100 K. Fig. 8 shows the changes in the capacitance values upon hydrogenation via remote H-plasma, RBA treatment and unbiased annealing in the temperature range 270-320 K. Each treatment was done for 20 minutes after which measurements were carried out with both -5 V and -2 V bias voltages.

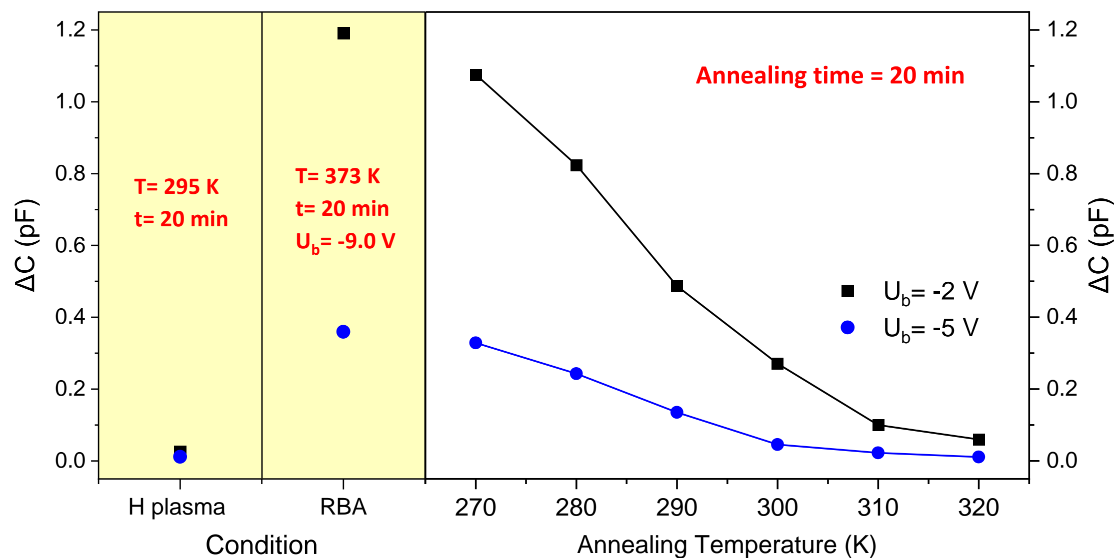

Fig. 8. Changes in the capacitance of the depletion region recorded via LDLTS on a diode fabrication on Si:P+B sample upon hydrogenation via remote H plasma at RT, RBA at 100°C, and isochronal annealing in the range 270-320 K in steps of 10 K for 20 minutes each with bias voltages of -5 V (blue) and -2 V (red).

The first clear observation in Fig. 8 is that the concentration of the BH_2 complex is higher close to the surface (using the lower bias voltage), i.e. there is a distribution of the BH_2 complexes from the surface to the deeper bulk in agreement with the results presented in Ref. [26]. The reduction in the ΔC value proceeds when the sample is kept at 270 K for 20 minutes. As the temperature is increased in steps of 10 K, the reduction rate is accelerated. If the ΔC value at each point is thought of as percentage change relative to the value recorded at the previous annealing temperature, the rate of reduction in ΔC keep increasing as the temperature is increased. This reflects the less time it takes to dissociate all the available BH_2 complexes as the sample is annealed at higher temperatures in the presence of electrons. The recorded data has been used to determine the activation energy of

annealing by conducting Arrhenius analysis. The derived activation energy of annihilation is found to be E_A=0.4±0.03 eV. While more careful analysis is needed to derive a more accurate value, this gives an idea of the relatively low energy required to dissociate the formed BH_2 complex which can be achieved at room temperature. It should be noted, however, that the values of BH_2 dissociation rate and the activation energy of the process are likely to be dependent on the concentration of available electrons.

3.5 Acceptor-hydrogen interactions: relevance to LeTID

In light of the importance of hydrogen-acceptor interactions in the LeTID mechanism of Si solar cells, we would like to discuss our results in the context of other results in the literature on the subject. According to the findings reported above, we propose the following sequence of reactions: the treatment in remote hydrogen plasma introduced significant amounts of hydrogen close to the surface, initially negatively charged (H^-) in n-type Si. These hydrogen atoms are attached effectively to positively charged P atoms forming electrically inactive PH pairs, thus causing the observed decrease in the active N_D^+ values close to the surface. It is important to remember that hydrogen in Si is a negative U defect with an occupancy level at 0.3-0.4 eV below the conduction band edge [34]. The subsequent application of the RBA treatment at 100 °C provides the necessary energy to release hydrogen from PH complexes and at the same time causes the Fermi level shift to the middle of the energy gap. Under these conditions, H atoms emit electrons and transform to the positively charged state (H^+) given the fact that its respective donor and acceptor levels are asymmetric with respect to the intrinsic level. This induces the Coulombic attraction of free H^+ atoms by the available negatively charged acceptor atoms B^- or Ga^-. The BH and GaH pairs are effective traps for available H^+ atoms [26], and as the $\mathrm{H}^+ + A\mathrm{H} \rightarrow A\mathrm{H}_2^+$ reactions are energetically favourable, electrically active BH_2 and GaH_2 complexes are formed. As long as no electrons are available, both BH_2 and GaH_2 complexes are stable at room temperature. The dissociation of the complexes is triggered by the presence of electrons which seems to lead first to the dissociation of the one hydrogen atom from the complex followed by the interaction of freed hydrogen, partly with phosphorus atoms to form PH pairs, and possibly with other available sinks including samples surfaces.

Three key elements play a major role in the LeTID defect formation/annihilation: atomic hydrogen, hydrogen dimers and AH pairs. Any factor affecting LeTID kinetics such as firing conditions can be understood as the modification of the population of one or more of these species. The LeTID triggering conditions, i.e. dark annealing or light soaking at elevated temperatures, induce different interactions between them. In our study, the simplest view is that the manipulation of these interactions has been utilized by either RBA which achieves a similar effect to the one expected from the light soaking treatment by inducing changes to the Fermi level position, or dark annealing at a certain temperature to overcome the energy barrier for several reactions. Detailed explanation of the formation and dissociation properties of the BH_2 complex, both in the dark and in the presence of minority carriers, has been carrier out and reported in ref. [35]. It is evident that the type of the acceptor species will also influence the degradation mechanism by forming acceptor-hydrogen complexes with different properties. This is also apparent in this work via the remarkable difference in the electronic properties of formed complexes when the acceptor atom is changed from B to Ga. The proposal that the LeTID defect consists of an acceptor atom connected to a complex incorporating some form of hydrogen atoms has been suggested recently by Kwapil *et al.* [7]. Even in n-type Si, it has been hypothesized that the lower susceptibility to LeTID can be explained by the different interactions between hydrogen and either boron or phosphorus atoms [48] and from our work potentially by different properties of BH_2 and PH_2.

Models to describe the degradation mechanism via hydrogen, whether 3-state or 4-state [49], are based on the interactions between the three species with the addition of more species like metallic impurities in some models [50]. Two main type of models have been proposed to explain the formation of the LeTID defect: 1) **association model** by which the LeTID defect precursor is available in the material after quenching fired samples and under the LeTID treatment, it interacts with hydrogen to form the recombination active complex, and 2) **dissociation model** by which the LeTID defect precursor consists of the LeTID defect connected to hydrogen, and the LeTID treatment plays the role of dissociating hydrogen from the defect precursor leading to the activation of the LeTID defect. From a first observation, our experimental and theoretical findings support the association model.

The previous evidence supporting the association model mainly attribute the defect activation to the hydrogen connection to the defect precursor, a step which should be preceded by the dissociation of H_2 dimers. The suggestion about the dissociation of the H_2 dimers was supported by the simultaneous decrease in the minority carrier lifetime and the increase in the BH pair concentration [21] based on the idea that H_2 supplies hydrogen to both, the LeTID defects and the BH pair formation. Another opinion was given also in the literature which attributes the defect activation to hydrogen interaction with defect precursor but this time the source of hydrogen is the dissociated BH pairs instead of H_2 under the degradation treatment [51]. Recently, the occurrence of maximum degradation has been proved to happen prior to BH pairs reaching maximum concentration value [52]. Such observation can be understood as the formation of LeTID defect and BH at the same time, via the association model, with the former being faster [52]. In our perspective, the formation of the BH_2 defect, responsible for LeTID, does not require the dissociation of the H_2 first, but rather occurs via the direct interaction of the H_2 dimers with available boron atoms. This opinion is very consistent with the new results of Hammann et al. [52] by which the formation of BH_2 defect can be linked with the faster increase in LeTID defect concentration compared to the increase in concentration of BH pairs. Even more convincing is the observed steep increase in BH concentration during the regeneration stage, explained by the dissociation of the BH_2 complex and further interaction of the released H atoms with available boron atoms.

Regarding the BH_2-related recombination mechanism in a p-type Si material, given the donor character of the complex with high capture cross section for electrons, the capture of photo-generated electron from the conduction band is a very efficient process. Next, being in the D^0 state, the BH_2 defect can: i) emit the capture electron back to the conduction band, ii) capture a hole from the valence band, or iii) transform from the D^0 state to the neutral acceptor state. In the first scenario, the BH_2 can be thought of as an electron trap. However, the latter two scenarios correspond to a recombination event either via a single defect level or via structural reconfiguration of the defect, respectively after which the defect returns back to the D^+ state eventually. The dominating scenario is determined by the rate of the possible transitions upon the capture of photo-generated electrons which itself is controlled by several parameters such as energy barriers. Our calculations indicate that the third scenario by which the defect reconfigure into A^0 state is much faster than the other two possibilities. Thus, our suggestion is that BH_2 is not a typical Shockley–Read–Hall recombination centre with a static level near mid-gap. Instead, its high recombination efficiency is justified from a dynamic electronic structure along a 3-step recombination mechanism summarized as: $D^+ + e^- + h^+ \rightarrow D^0 + h^+ \rightarrow A^0 + h^+ \rightarrow D^+$. This is supported by the relatively high concentration of H atoms and the small jumps needed to achieve the proposed reactions.

The picture for LeTID in Ga-doped Si is not fully understood at the moment. Under the conditions of the present study, the GaH_2 defect cannot account for the lifetime degradation in Ga-doped Si.

However, this study is consistent with previous reports in the way that Ga-LeTID is certainly different from that occurring in the B case. The specific conditions that are needed to trigger degradation in Ga-doped Si solar cells could mean that the treatments we have applied in this study are not the ones relevant to the creation of recombination centres in Ga-doped material. Further, there is no solid evidence in the literature that LeTID in Ga-doped and in B-doped Si is related to the same defect.

All of the above does not necessarily eliminate the involvement of other species such as metallic impurities in the degradation mechanism or the existence of more species (such as hydrogen sinks) which can alter the reactions kinetics between H_2, BH_2 and BH.

Summary:

The significance of understanding reactions involving hydrogen atoms and group-III acceptors lies on their primary role in the occurrence of LeTID of Si solar cells and in the urgency of deriving a solution for it. These interactions were provoked via remote H plasma treatments, and investigated experimentally by means of CV, DLTS, Laplace DLTS, and theoretically by density functional calculations. Hydrogen-acceptor reactions were triggered via reverse bias annealing and conventional annealing treatments of diodes made on Si:P+B and Si:P+Ga materials.

It has been argued that a complex comprising one boron atom and two hydrogen atoms is formed upon the interactions of available positively charged hydrogen atoms with boron or gallium atoms. The BH_2 complex has a donor level close to 0.18 eV below the conduction band and we propose that this could be an effective recombination centre for minority carriers in p-type material. The analysis of defect formation and annihilation kinetics shows that the complex can account for several LeTID-related observation in the literature. The similar changes in the donor concentration profiles in the hydrogenated Si:P+Ga and Si:P+B indicate that formation of GaH_2 and BH_2 occur via analogous processes. Even if the interactions between hydrogen and B and Ga are similar, the electronic properties of the formed complexes are very different, whereby GaH_2 is found to possess a shallow level confirmed via theoretical and experimental results and is thus an electron trap with weak recombination activity. The GaH_2 complex was found to be more thermally stable than the BH_2 one, in similarity to the same trend for the acceptor-hydrogen pairs. Our annealing results indicate that the annihilation of both complexes requires the availability of electrons. While our results do not eliminate the involvement of other species, the interactions between hydrogen dimers, acceptor-dihydrogen complexes and acceptor-hydrogen pairs are suggested to be in the heart of the LeTID mechanism.

Declaration of competing interest:

The authors declare that they have no known competing financial interests or personal relationships that could have appeared to influence the work reported in this paper.

Data Availability Statement:

The data that support the findings of this study are available from the corresponding author upon reasonable request

Acknowledgments:

This work was supported in the UK by EPSRC project EP/T025131/1. J.C. acknowledges the FCT through projects LA/P/0037/2020, UIDB/50025/2020, UIDP/50025/2020 and 2021.09643.CPCA (Advanced Computing Project using the Oblivion supercomputer).

References:

[1] N.E. Grant, P.P. Altermatt, T. Niewelt, R. Post, W. Kwapil, M.C. Schubert, J.D. Murphy, Gallium-Doped Silicon for High-Efficiency Commercial Passivated Emitter and Rear Solar Cells, Solar RRL, 5 (2021) 2000754. https://doi.org/10.1002/solr.202000754.
[2] G. Fischer, F. Wolny, H. Neuhaus, M. Müller, Aspects of Gallium Doping for PERC Solar Cells, in: 37th European Photovoltaic Solar Energy Conference and Exhibition Germany, 2020, pp. 11.
[3] S. Zhang, J. Peng, H. Qian, H. Shen, Q. Wei, W. Lian, Z. Ni, J. Jie, X. Zhang, L. Xie, The impact of thermal treatment on light-induced degradation of multicrystalline silicon PERC solar cell, Energies, 12 (2019) 416. https://doi.org/10.3390/en12030416.
[4] N.E. Grant, J.R. Scowcroft, A.I. Pointon, M. Al-amin, P.P. Altermatt, J.D. Murphy, Lifetime instabilities in gallium doped monocrystalline PERC silicon solar cells, Sol. Enegry Mater. Sol. Cells, 206 (2020) 110299. https://doi.org/10.1016/j.solmat.2019.110299.
[5] D. Lin, Z. Hu, L. Song, D. Yang, X. Yu, Investigation on the light and elevated temperature induced degradation of gallium-doped Cz-Si, Sol. Energy, 225 (2021) 407-411. https://doi.org/10.1016/j.solener.2021.07.023.
[6] J.M. Fritz, A. Zuschlag, D. Skorka, A. Schmid, G. Hahn, Temperature dependent degradation and regeneration of differently doped mc-Si materials, Energy Proc., 124 (2017) 718-725. https://doi.org/10.1016/j.egypro.2017.09.085.
[7] W. Kwapil, J. Dalke, R. Post, T. Niewelt, Influence of Dopant Elements on Degradation Phenomena in B- and Ga-Doped Czochralski-Grown Silicon, Solar RRL, 5 (2021) 2100147-2100147. https://doi.org/10.1002/solr.202100147.
[8] S. Jafari, M. Figg, Z. Hameiri, Investigation of light-induced degradation in gallium- and indium-doped Czochralski silicon, Sol. Enegry Mater. Sol. Cells, 251 (2023) 112121. https://doi.org/10.1016/j.solmat.2022.112121.
[9] D. Chen, M. Vaqueiro Contreras, A. Ciesla, P. Hamer, B. Hallam, M. Abbott, C. Chan, Progress in the understanding of light- and elevated temperature-induced degradation in silicon solar cells: A review, Prog. Photovoltaic Res. Appl., 29 (2020) 1180-1201. https://doi.org/10.1002/pip.3362.
[10] D. Chen, M. Kim, B.V. Stefani, B.J. Hallam, M.D. Abbott, C.E. Chan, R. Chen, D.N.R. Payne, N. Nampalli, A. Ciesla, T.H. Fung, K. Kim, S.R. Wenham, Evidence of an identical firing-activated carrier-induced defect in monocrystalline and multicrystalline silicon, Sol. Enegry Mater. Sol. Cells, 172 (2017) 293-300. https://doi.org/10.1016/j.solmat.2017.08.003.
[11] R. Eberle, W. Kwapil, F. Schindler, M.C. Schubert, S.W. Glunz, Impact of the firing temperature profile on light induced degradation of multicrystalline silicon, Phys. Status Solidi Rapid Res. Lett., 10 (2016) 861-865. https://doi.org/10.1002/pssr.201600272.
[12] C. Sen, M. Kim, D. Chen, U. Varshney, S. Liu, A. Samadi, A. Ciesla, S.R. Wenham, C.E. Chan, C. Chong, M.D. Abbott, B.J. Hallam, Assessing the Impact of Thermal Profiles on the Elimination of Light- and Elevated-Temperature-Induced Degradation, IEEE J. Photovoltaics, 9 (2019) 40-48. https://doi.org/10.1109/jphotov.2018.2874769.
[13] U. Varshney, M.D. Abbott, S. Liu, D. Chen, M. Kim, C. Sen, D.N.R. Payne, S.R. Wenham, B. Hoex, C. Chan, Influence of dielectric passivation layer thickness on LeTID in multicrystalline silicon, in: 7th World Conference on Photovoltaic Energy Conversion (WCPEC), IEEE, 2018, pp. 0363-0367.
[14] U. Varshney, M. Abbott, A. Ciesla, D. Chen, S. Liu, C. Sen, M. Kim, S. Wenham, B. Hoex, C. Chan, Evaluating the Impact of SiNx Thickness on Lifetime Degradation in Silicon, IEEE J. Photovoltaics, 9 (2019) 601-607. https://doi.org/10.1109/jphotov.2019.2896671.
[15] A. Schmid, C. Fischer, D. Skorka, A. Herguth, C. Winter, A. Zuschlag, G. Hahn, On the Role of AlOx Thickness in AlOx/SiNy:H Layer Stacks Regarding Light- and Elevated Temperature-Induced

Degradation and Hydrogen Diffusion in c-Si, IEEE J. Photovoltaics, 11 (2021) 967-973. https://doi.org/10.1109/jphotov.2021.3075850.
[16] U. Varshney, M. Kim, M.U. Khan, P. Hamer, C. Chan, M. Abbott, B. Hoex, Impact of Substrate Thickness on the Degradation in Multicrystalline Silicon, IEEE J. Photovoltaics, 11 (2021) 65-72. https://doi.org/10.1109/jphotov.2020.3038412.
[17] D. Bredemeier, D.C. Walter, J. Schmidt, Possible Candidates for Impurities in mc-Si Wafers Responsible for Light-Induced Lifetime Degradation and Regeneration, Solar RRL, 2 (2018) 1700159. https://doi.org/10.1002/solr.201700159.
[18] D. Chen, P. Hamer, M. Kim, C. Chan, A. Ciesla nee Wenham, F. Rougieux, Y. Zhang, M. Abbott, B. Hallam, Hydrogen-induced degradation: Explaining the mechanism behind light- and elevated temperature-induced degradation in n- and p-type silicon, Sol. Enegry Mater. Sol. Cells, 207 (2020) 110353. https://doi.org/10.1016/j.solmat.2019.110353.
[19] T.H. Fung, M. Kim, D. Chen, A. Samadi, C.E. Chan, B.J. Hallam, S. Wenham, M. Abbott, Influence of bound hydrogen states on carrier-induced degradation in multi-crystalline silicon, in: AIP Conference Proceedings, 2018, pp. 130004.
[20] C. Winter, J. Simon, A. Herguth, Study on Boron–Hydrogen Pairs in Bare and Passivated Float-Zone Silicon Wafers, Phys. Status Solidi A, 218 (2021) 2100220. https://doi.org/10.1002/pssa.202100220.
[21] B. Hammann, L. Rachdi, W. Kwapil, F. Schindler, M.C. Schubert, Insights into the Hydrogen-Related Mechanism behind Defect Formation during Light- and Elevated-Temperature-Induced Degradation, Phys. Status Solidi Rapid Res. Lett., 15 (2021) 2000584. https://doi.org/10.1002/pssr.202000584.
[22] V.V. Voronkov, R. Falster, Formation, dissociation, and diffusion of various hydrogen dimers in silicon, Phys. Status Solidi B, 254 (2017) 1600779. https://doi.org/10.1002/pssb.201600779.
[23] V.V. Voronkov, Independent Subsystems of Atomic Hydrogen in Silicon Responsible for Boron Passivation and for Dimer Production, Phys. Status Solidi A, 219 (2022) 2200081. https://doi.org/10.1002/pssa.202200081.
[24] T.O. Abdul Fattah, V.P. Markevich, J.A.T. De Guzman, J. Coutinho, S.B. Lastovskii, I.D. Hawkins, I.F. Crowe, M.P. Halsall, A.R. Peaker, Interactions of Hydrogen Atoms with Acceptor–Dioxygen Complexes in Czochralski-Grown Silicon, Phys. Status Solidi A, (2022) 2200176. https://doi.org/10.1002/pssa.202200176.
[25] W. Kwapil, J. Dalke, T. Niewelt, M.C. Schubert, LeTID-and (extended) BO-related degradation and regeneration in B-and Ga-doped monocrystalline silicon during dark and illuminated anneals, in: 37th European PV Solar Energy Conference and Exhibition, 2020, pp. 11.
[26] J.A.T. De Guzman, V.P. Markevich, J. Coutinho, N.V. Abrosimov, M.P. Halsall, A.R. Peaker, Electronic Properties and Structure of Boron–Hydrogen Complexes in Crystalline Silicon, Solar RRL, (2021) 2100459. https://doi.org/10.1002/solr.202100459.
[27] A.R. Peaker, V.P. Markevich, J. Coutinho, Junction spectroscopy techniques and deep-level defects in semiconductors, J. Appl. Phys., 123 (2018) 161559-161559. https://doi.org/10.1063/1.5011327.
[28] G. Kresse, J. Furthmüller, Efficiency of ab-initio total energy calculations for metals and semiconductors using a plane-wave basis set, Comput.l Mater. Sci., 6 (1996) 15-50. https://doi.org/10.1016/0927-0256(96)00008-0.
[29] G. Kresse, J. Hafner, Ab initio molecular dynamics for liquid metals, Phys. Rev. B, 47 (1993) 558. https://doi.org/10.1103/PhysRevB.47.558.
[30] P.E. Blochl, Projector augmented-wave method, Phys. Rev. B, 50 (1994) 17953-17979. https://doi.org/10.1103/PhysRevB.50.17953.
[31] J. Heyd, G.E. Scuseria, M. Ernzerhof, Hybrid functionals based on a screened Coulomb potential, J. Chem. Phy., 118 (2003) 8207-8215. https://doi.org/10.1063/1.1564060.
[32] J.P. Perdew, K. Burke, M. Ernzerhof, Generalized Gradient Approximation Made Simple, Phys. Rev. Lett., 77 (1996) 3865-3868. https://doi.org/10.1103/PhysRevLett.77.3865.

[33] C. Freysoldt, J. Neugebauer, C.G. Van de Walle, Fully Ab Initio Finite-Size Corrections for Charged-Defect Supercell Calculations, Phys. Rev. Lett., 102 (2009) 016402-016402. https://doi.org/10.1103/PhysRevLett.102.016402.
[34] D. Gomes, V.P. Markevich, A.R. Peaker, J. Coutinho, Dynamics of Hydrogen in Silicon at Finite Temperatures from First Principles, Phys. Status Solidi B, 259 (2022) 2100670. https://doi.org/10.1002/pssb.202100670.
[35] J. Coutinho, D. Gomes, V.J.B. Torres, T.O. Abdul Fattah, V.P. Markevich, A.R. Peaker, Theory of reactions between hydrogen and group-III acceptors in silicon, (unpublished results).
[36] N.M. Johnson, C. Herring, D.J. Chadi, Interstitial hydrogen and neutralization of shallow-donor impurities in single-crystal silicon, Phys. Rev. Lett., 56 (1986) 769. https://doi.org/10.1103/PhysRevLett.56.769.
[37] L. Korpás, J.W. Corbett, S.K. Estreicher, Multiple trapping of hydrogen at boron and phosphorus in silicon, Phys. Rev. B, 46 (1992) 12365. https://doi.org/10.1103/PhysRevB.46.12365.
[38] M. Vaqueiro-Contreras, V.P. Markevich, J. Mullins, M.P. Halsall, L.I. Murin, R. Falster, J. Binns, J. Coutinho, A.R. Peaker, Lifetime degradation of n-type Czochralski silicon after hydrogenation, J. Appl. Phys., 123 (2018) 161415. https://doi.org/10.1063/1.5011351.
[39] M. Vaqueiro-Contreras, V.P. Markevich, M.P. Halsall, A.R. Peaker, P. Santos, J. Coutinho, S. Öberg, L.I. Murin, R. Falster, J. Binns, E.V. Monakhov, B.G. Svensson, Powerful recombination centers resulting from reactions of hydrogen with carbon-oxygen defects in n-type Czochralski-grown silicon, Phys. Status Solidi Rapid Res. Lett., 11 (2017) 1700133. https://doi.org/10.1002/pssr.201700133.
[40] R. Stübner, V. Kolkovsky, J. Weber, Two different carbon-hydrogen complexes in silicon with closely spaced energy levels, J. Appl. Phys., 118 (2015) 055704. https://doi.org/10.1063/1.4928146.
[41] R. Stübner, V. Kolkovsky, J. Weber, N.V. Abrosimov, C.M. Stanley, D.J. Backlund, S.K. Estreicher, Identification of the donor and acceptor states of the bond-centered hydrogen–carbon pair in Si and diluted SiGe alloys, J. Appl. Phys., 127 (2020) 045701. https://doi.org/10.1063/1.5135757.
[42] A. Endros, Charge-state-dependent hydrogen-carbon-related deep donor in crystalline silicon, Phys. Rev. Lett., 63 (1989) 70. https://doi.org/10.1103/PhysRevLett.63.70.
[43] A.L. Endrös, W. Krühler, F. Koch, Electronic properties of the hydrogen-carbon complex in crystalline silicon, J. Appl. Phys., 72 (1992) 2264-2271. https://doi.org/10.1063/1.351620.
[44] A.R. Peaker, V.P. Markevich, L. Dobaczewski, Defects in microelectronic materials and devices, CRC press, Boca Raton, 2008.
[45] P.J.H. Denteneer, C.G. Van de Walle, S.T. Pantelides, Microscopic structure of the hydrogen-boron complex in crystalline silicon, Phys. Rev. B, 39 (1989) 10809. https://doi.org/10.1103/PhysRevB.39.10809.
[46] N.M. Johnson, Mechanism for hydrogen compensation of shallow-acceptor impurities in single-crystal silicon, Phys. Rev. B, 31 (1985) 5525. https://doi.org/10.1103/PhysRevB.31.5525.
[47] J.I. Pankove, D.E. Carlson, J.E. Berkeyheiser, R.O. Wance, Neutralization of shallow acceptor levels in silicon by atomic hydrogen, Phys. Rev. Lett., 51 (1983) 2224. https://doi.org/10.1103/PhysRevLett.51.2224.
[48] W. Kwapil, J. Schon, T. Niewelt, M.C. Schubert, Temporary Recovery of the Defect Responsible for Light- and Elevated Temperature-Induced Degradation: Insights Into the Physical Mechanisms Behind LeTID, IEEE J. Photovoltaics, 10 (2020) 1591-1603. https://doi.org/10.1109/jphotov.2020.3025240.
[49] T.H. Fung, M. Kim, D. Chen, C.E. Chan, B.J. Hallam, R. Chen, D.N.R. Payne, A. Ciesla, S.R. Wenham, M.D. Abbott, A four-state kinetic model for the carrier-induced degradation in multicrystalline silicon: Introducing the reservoir state, Sol. Enegry Mater. Sol. Cells, 184 (2018) 48-56. https://doi.org/10.1016/j.solmat.2018.04.024.
[50] J. Schmidt, D. Bredemeier, D.C. Walter, On the Defect Physics Behind Light and Elevated Temperature-Induced Degradation (LeTID) of Multicrystalline Silicon Solar Cells, IEEE J. Photovoltaics, 9 (2019) 1497-1503. https://doi.org/10.1109/JPHOTOV.2019.2937223.

[51] D.C. Walter, D. Bredemeier, V.V. Voronkov, R. Falster, J. Schmidt, Disappearance of hydrogen-boron-pairs in silicon during illumination and its relevance to lifetime degradation and regeneration effects in solar cells, in: 37th European Photovoltaic Solar Energy Conference and Exhibition, 2020.
[52] B. Hammann, N. Assmann, P.M. Weiser, W. Kwapil, T. Niewelt, F. Schindler, R. Sondena, E.V. Monakhov, M.C. Schubert, The Impact of Different Hydrogen Configurations on Light- and Elevated-Temperature- Induced Degradation, IEEE J. Photovoltaics, 13 (2023) 224-235. https://doi.org/10.1109/jphotov.2023.3236185.